LETTER

Realizing multiple-qubit entangling gate in Rydberg atoms via soft quantum control

To cite this article: Meng-Ru Yun *et al* 2022 *EPL* **140** 58003

A Letters Journal Exploring the Frontiers of Physics

December 2022

EPL, **140** (2022) 58003
doi: 10.1209/0295-5075/aca69a

www.epljournal.org

Realizing multiple-qubit entangling gate in Rydberg atoms via soft quantum control

Meng-Ru Yun[1(a)], Shuming Cheng[2,3,4(b)], L.-L. Yan[1,5(c)], Y. Jia[6,1(d)] and S.-L. Su[1,5]

[1] *International Laboratory for Quantum Functional Materials of Henan, and School of Physics and Microelectronics, Zhengzhou University - Zhengzhou 450001, China*
[2] *The Department of Control Science and Engineering, Tongji University - Shanghai 201804, China*
[3] *Shanghai Institute of Intelligent Science and Technology, Tongji University - Shanghai 201804, China*
[4] *Institute for Advanced Study, Tongji University - Shanghai, 200092, China*
[5] *School of Physics and Microelectronics, Key Laboratory of Materials Physics of Ministry of Education, Zhengzhou University - Zhengzhou 450001, China*
[6] *Key Laboratory for Special Functional Materials of Ministry of Education, and School of Materials and Engineering, Henan University - Kaifeng 475001, China*

received 11 March 2022; accepted in final form 28 November 2022
published online 7 December 2022

Abstract – Entangling gates are important for the generation of entanglement in quantum communicational and computational tasks. In this work, we propose an efficient protocol to realize the multi-qubit entangling gates with high fidelity in Rydberg atoms. Particularly, we apply the technique of soft quantum control to design the off-resonant pulses such that the atoms are driven to the ground-state subspace via unconventional Rydberg pumping. Thus, our scheme is insensitive to the decay effect as all atoms are only virtually excited. Moreover, Gaussian temporal modulation is further adopted to improve its robustness against the model uncertainty, such as operating time and environment noise. Finally, we perform numerical simulation to validate the effectiveness of our scheme. Hence, our work has potential applications in quantum information processing based on Rydberg atoms.

Introduction. – Entanglement, as a fundamental feature of quantum mechanics, plays an important role in quantum information processing (QIP), such as quantum cryptography [1,2], dense coding [3,4], teleportation [5,6], distributed quantum computation [7,8], quantum secret sharing [9,10] and so on [11–15]. Especially, for quantum networks, preparing entangling gates with high efficiency and fidelity are urged by the rapid development of quantum technology [16–19]. Although entangling gates are usually realized by implementing a series of single- and two-qubit gates [20], this typically consumes exponential resources as the number of qubits goes large [21]. For example, the implementation of three-qubit Toffoli gate requires five two-qubit gates at least and an extra set of single-qubit gates [22]. Besides, error will accumulate in the whole process, thus hindering the realization of multiple-qubit entangling gates with high fidelity. Thus, preparing multiple-qubit entangled gate by one step is highly demanding. Correspondingly, many methods have been proposed for the preparation of multiple-qubit states in various physical platforms, such as superconducting circuits [23,24], circuit QED [25], trapped ion [26], neutral atom [27–31], and so on [32].

Rydberg atoms, with a valence electron excited to high-lying Rydberg state [33], have been regarded as one of the most competitive candidates for quantum computation and simulation due to their long coherence time and strong Rydberg-Rydberg interaction (RRI) [34]. Specifically, the dipole-dipole interaction, together with van der Waals interaction, lead to an interesting phenomenon known as the Rydberg blockade [35–37] that if a Rydberg atom is excited to the Rydberg state, then the excitation of other atoms in the same volume will be suppressed. Based on this phenomenon, many schemes have been proposed to realize quantum logic gates [38–51], quantum entanglement [27,39,50,52–60], and QIP [61–63]. Furthermore, the Rydberg antiblockade regime has also been explored where more than one Rydberg atom can be be excited

(a) E-mail: mengruYun@163.com (corresponding author)
(b) E-mail: shuming_cheng@tongji.edu.cn
(c) E-mail: llyan@zzu.edu.cn
(d) E-mail: jiayu@zzu.edu.cn

simultaneously [64], with experimental demonstration reported in [65] and wide applications in realizing quantum logic gates [28,66–68], and so on [69]. However, both the Rydberg blockade and Rydberg antiblockade depend on whether an atom is in Rydberg state.

To avoid the above issue, the technique of unconventional Rydberg pumping (URP) could be used to freeze the evolution of system if two atoms are in the same ground state [70]. Besides, Haase *et al.* [71] proposed the technique of soft quantum control, which allows to perform an efficient rotating-wave approximation (RWA) in a wide parameter regime. The soft quantum control has been used in state preparation [72], construction of quantum gates [73], quantum sensing [74,75], and so on. Here, we use this technique to suppress the unwanted high-frequency oscillations and parameter uncertainty during the preparation process, thus improving the gate fidelity.

In this work, we present an efficient method to directly realize three-qubit entangling gates in Rydberg atoms. In particular, we employ the off-resonant driving strategy [76], which is able to eliminate the Stark shift to fit the effective Hamiltonian and full Hamiltonian very well. Finally, by modeling the noise in the form of the Lindblad master equations, we investigate the gate performance of our scheme in terms of the state fidelity and the average fidelity based on the trace-preserving quantum operator, respectively. It is found that our method achieves the gate fidelity up to above 99.6% at least.

The paper is organized as follow. In section "Physical model and effective Hamiltonian", the effective Hamiltonian for the interacting Rydberg atoms is first derived, and the corresponding three-qubit entangling gates are generated based on this Hamiltonian. Then, the performance of the multiple-qubit entangling gate is analyzed in section "Analysis of the gate fidelity". In order to improve the gate fidelity, we apply the soft quantum control technique to fight against noise induced by decay and dephasing in the form of the master equation in section "Gate fidelity with soft quantum control". Finally, we conclude with our work in section "Conclusion".

Physical model and effective Hamiltonian. – We choose ^{87} Rb atoms as the physical platform where two ground energy levels are $|0\rangle = |5S_{1/2}, F = 1, m_F = 0\rangle$ and $|1\rangle = |5S_{1/2}, F = 2, m_F = 0\rangle$ respectively, and the Rydberg state is denoted by $|r\rangle = |100S_{1/2}, m_J = 1/2\rangle$. Indeed, the excitation of an even-parity Rydberg state with the principal quantum number around 100has been observed in refs. [77–79]. As illustrated in fig. 1, we consider the scenario where the left atom, labelled as atom 1, is the control atom and the rest labelled as atom 2 and 3 in the right side are the target. Specifically, the Rydberg state of atom 1 is coupled to its ground state $|0\rangle$ by classical lasers with Rabi frequency Ω_0, with detuning Δ. The other laser with same Rabi frequency Ω_0 and the detuning Δ with opposite sign is introduced to eliminate the Shark shift, and atom 2 and atom 3 are driven by classical lasers

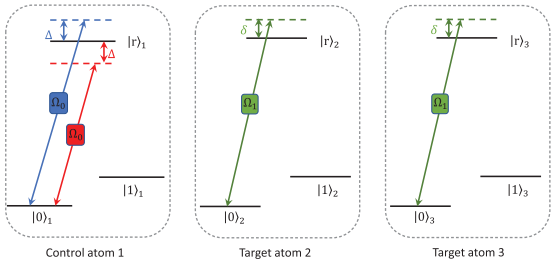

Fig. 1: The energy level configuration of control atom 1, target atom 2 and target atom 3. $|0\rangle$ and $|1\rangle$ are ground states, and $|r\rangle$ is the Rydberg state. Atom 1 is the control atom, driven by two lasers with Rabi frequency Ω_0, detuned by Δ and $-\Delta$. Atom 2 and atom 3 are target atoms that driven by lasers with Rabi frequency Ω_1, detuned by $-\delta$.

with Rabi frequency Ω_1 and detuning δ. By the way, the optical tweezers which are used to trap the Rydberg atoms have to be switched off during operation to prevent Rydberg atoms from being influenced by other lights [80,81].

In the interaction picture, the Hamiltonian of this system can be written as ($\hbar = 1$)

$$H_I = 2\Omega_0 \cos(\Delta t)|0\rangle_1\langle r| + \sum_{n=2}^{3} \Omega_1 |0\rangle_n\langle r| e^{i\delta t} + \text{H.c.} + \sum_{j\neq k} V_{jk}|rr\rangle_{jk}\langle rr|. \quad (1)$$

Here, $V_{jk} = C_6/R^6$ describes the van der Waals interaction between the j-th atom and the k-th atom where R is the distance between Rydberg atoms and C_6 depends on the quantum numbers of the Rydberg state, such as $C_6/2\pi = 56.2\,\text{THz}\cdot\mu\text{m}^6$ for ^{87} Rb [42,82,83]. And the parameters can be chosen as $\delta = 2\pi \times 1\,\text{MHz}$, $V_{12} = V_{13} = 2\pi \times 101\,\text{MHz}$, $V_{23} = 2\pi \times 101/8\,\text{MHz}$, $\Delta = 2\pi \times 100\,\text{MHz}$ $\Omega_0 = 2\pi \times 2\,\text{MHz}$ and $\Omega_1 = 2\pi \times 0.05\,\text{MHz}$ [84].

Further, we apply the rotating frame with respect to $U = \exp(-it\sum_{j\neq k} V_{jk}|rr\rangle_{jk}\langle rr|)$ to the above Hamiltonian as per eq. (1) and can obtain

$$\begin{aligned}\tilde{H}_I &= i\dot{U}^\dagger U + U^\dagger H_I U \\ &\approx |0\rangle\langle 0| \otimes H_0 + |1\rangle\langle 1| \otimes H_1 \\ &\quad + (|0\rangle\langle r| \otimes H_r + \text{H.c}),\end{aligned} \quad (2)$$

where $|0\rangle, |1\rangle, |r\rangle$ are states of the control atom and the corresponding Hamiltonian H_0, H_1, H_r are for atoms 2 and 3. Obviously, the whole Hamiltonian is decomposed into three parts, conditioned on the state of the control atom.

Particularly, if the control atom is $|0\rangle$, then we have

$$\begin{aligned}H_0 &= \Omega_1(|00\rangle\langle r0| + |00\rangle\langle 0r| + |01\rangle\langle r1| + |10\rangle\langle 1r|) + \text{H.c.} \\ &\quad -\delta(|r0\rangle\langle r0| + |r1\rangle\langle r1| + |0r\rangle\langle 0r| + |1r\rangle\langle 1r|),\end{aligned} \quad (3)$$

and the Hamiltonian H_r can be explicitly written as

$$H_r = \Omega_0(|0r\rangle\langle 0r| + |r0\rangle\langle r0| + |1r\rangle\langle 1r| + |r1\rangle\langle r1|), \quad (4)$$

where the RWA is used to eliminate the high-frequency oscillating terms and $V_{12} = V_{13} = \Delta + \delta$. Inspired by ref. [70], which is different from Rydberg blockade or Rydberg antiblockade, URP is closely related to the ground states of atoms by adjusting the relationship between the detuning and the Rabi frequency. Here, we set $\{\Omega_0, \delta\} \gg \Omega_1$, then the evolution will be trapped in the single-excited states $\{|00r\rangle, |0r0\rangle, |01r\rangle, |0r1\rangle\}$ and double-excited states $\{|r0r\rangle, |rr0\rangle, |r1r\rangle, |rr1\rangle\}$, and the eigenenergies of the dressed states are much larger than the transition between ground states and single-excited states so that the evolution will be frozen if the control atom is in state $|0\rangle$.

When the control atom is $|1\rangle$, there is

$$\begin{aligned} H_1 = \Omega_1(&|00\rangle\langle r0| + |00\rangle\langle 0r| + |01\rangle\langle r1| + |10\rangle\langle 1r|) \\ &+ \text{H.c.} - \delta(|\text{r0}\rangle\langle \text{r0}| + |\text{r1}\rangle\langle \text{r1}| + |\text{0r}\rangle\langle \text{0r}| \\ &+ |1r\rangle\langle 1r|). \end{aligned} \tag{5}$$

Furthermore, given $\delta \gg \Omega_1$, by using the J-J method [85], we can obtain the effective Hamiltonian from H_1 under the second-order perturbation theory,

$$H_{\text{eff}} = \frac{\Omega_1^2}{\delta}(2|00\rangle\langle 00| + |01\rangle\langle 01| + |10\rangle\langle 10|). \tag{6}$$

It follows from eq. (2) that if the URP condition is satisfied, we can see that there is no excitation of atoms, so the error caused by spontaneous emission can be ignored. Hence, the evolution is governed by

$$\hat{U}(t) = e^{-it\tilde{H}_I} = |0\rangle\langle 0| \otimes \hat{I} + |1\rangle\langle 1| \otimes \hat{U}_1, \tag{7}$$

where $\hat{I}$ is the identity operator and $\hat{U}_1 = \text{diag}[\text{e}^{-i\frac{2\Omega_1^2}{\delta}t}, \text{e}^{-i\frac{\Omega_1^2}{\delta}t}, \text{e}^{-i\frac{\Omega_1^2}{\delta}t}, 1]$ in the basis $\{|00\rangle_{23} = (1,0,0,0)^T, |01\rangle_{23} = (0,1,0,0)^T, |10\rangle_{23} = (0,0,1,0)^T, |11\rangle_{23} = (0,0,0,1)^T\}$. This immediately gives rise to a class of three-qubit entangling gates which are able to generate entanglement. We remark that the above proposal only requires tuning laser frequencies properly and need not implement a set of single- and two-qubit gates sequentially. Thus, it may provide an efficient approach to realize multi-qubit entangling gates.

Analysis of the gate fidelity. – In this section, we introduce two quantifiers to evaluate the gate performance of the method proposed in the above section. One is the state fidelity between the prepared states and targeted states, and the other is the average fidelity based on the trace-preserving quantum operator (TPQO) [86]. Moreover, the noise effect is modelled as the Lindbladian master equation, and then we analyze the noise robustness for the entangling gates generated via eq. (7).

Gate fidelity without soft quantum control. The three-atom system is initially prepared into the state $|\Psi(0)\rangle = 1/\sqrt{2}(|0\rangle_1 + |1\rangle_1) \otimes 1/\sqrt{2}(|0\rangle_2 + |1\rangle_2) \otimes 1/\sqrt{2}(|0\rangle_3 + |1\rangle_3)$.

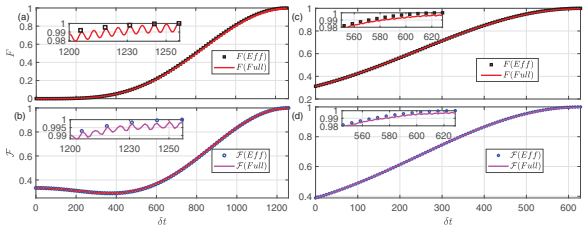

Fig. 2: The fidelity F ((a), (c)) and average fidelity $\mathcal{F}$ ((b), (d)) of the multiple-qubit entangling gate, where the black square (blue circle) and purple (black) solid line denote the fidelity based on the full Hamiltonian (eq. (1)) and the effective Hamiltonian (eq. (6)), the corresponding final state of (a), (b) is $|\Psi(\tau_1)\rangle$, and the corresponding final state of (c), (d) is $|\Psi(\tau_2)\rangle$, where $\Omega_0 = 2\delta$, $\Omega_1 = 0.05\delta$, $\Delta = 100\delta$, $V_{12} = V_{13} = 8V_{23} = 101\delta$.

After time $\tau_1(\tau_2)$ chosen as $\tau_1 = \pi/\overline{\Omega}_1(\tau_2 = \pi/2\overline{\Omega}_2)$ with $\overline{\Omega}_1 = \Omega_1^2/\delta(\overline{\Omega}_2 = \Omega_1^2/\delta)$, eq. (7) leads to

$$\begin{aligned} \hat{U}(\tau_1) &= \text{diag}[1,1,1,1,1,-1,-1,1], \\ \hat{U}(\tau_2) &= \text{diag}[1,1,1,1,-1,-i,-i,1]. \end{aligned} \tag{8}$$

Hence, genuine entangled states are prepared as $|\Psi(\tau_1)\rangle = 1/\sqrt{8}(|000\rangle + |010\rangle + |001\rangle + |011\rangle + |100\rangle - |101\rangle - |110\rangle + |111\rangle)(|\Psi(\tau_2)\rangle = 1/\sqrt{8}(|000\rangle + |010\rangle + |001\rangle + |011\rangle - |100\rangle - i|101\rangle - i|110\rangle + |111\rangle))$ (the entanglement details of $|\Psi(\tau_1)\rangle(|\Psi(\tau_2)\rangle)$ are given in the appendix). Thus, the gate performance is evaluated via the state fidelity [87]

$$F = \langle\Psi(\tau)|\rho(t)|\Psi(\tau)\rangle, \tag{9}$$

where $\rho(t)$ is the evolution density matrix. On the other hand, we introduce average fidelity based on the trace-preserving quantum operator (TPQO) [86] defined as

$$\mathcal{F}(\epsilon, \mathcal{O}) = \left[\sum_j \text{tr}(\mathcal{O}\mathcal{O}_j^\dagger \mathcal{O}^\dagger \epsilon(\mathcal{O}_j)) + d^2\right] / d^2(d+1), \tag{10}$$

where $\mathcal{O}_j$ is the tensor of Pauli matrices $III, IIX, \ldots, ZZZ$; $\mathcal{O}$ is the perfect entangling gate, $d = 8$ for a three-atom quantum logic gate and ϵ is the trace-preserving quantum operation achieved through our scheme.

We plot the time evolutions of fidelity F and average fidelity $\mathcal{F}$ by solving the Schrödinger equation in fig. 2(a) and fig. 2(b), where the fidelity F and average fidelity $\mathcal{F}$ of 99.77% (99.64%) and 99.8% (99.7%) of the full Hamiltonian equation (1) can be achieved for $\hat{U}(\tau_1)$ ($\hat{U}(\tau_2)$), respectively, and the effective Hamiltonian fits the full Hamiltonian very well.

Gate fidelity with soft quantum control. From fig. 2, we can see that there are obvious oscillations when we achieve this multiple-qubit entangling gate. These oscillations caused by the imperfection of parameter selection make the scheme sensitive to the operation time errors, *i.e.*, the standard method achieves high fidelity only for discrete values of time. Haase *et al.* [71] proposed the

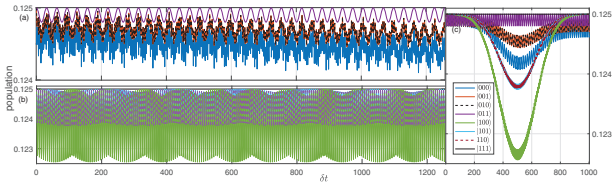

Fig. 3: The population of $|000\rangle$, $|001\rangle$, $|010\rangle$, $|011\rangle$, $|100\rangle$, $|101\rangle$, $|110\rangle$, and $|111\rangle$, its evolution operator is $U(\tau_1)$, and the same is true for $U(\tau_2)$. The Rabi frequency of (a), (b) is driven by the standard method, and (c) is driven by the soft quantum control, where parameters are the same as fig. 2.

technique of soft quantum control, which allows to perform an efficient rotating-wave approximation (RWA) in a wide parameter regime. In soft quantum control, the Rabi frequency is small at the beginning and at the end of quantum evolution, unwanted transitions would be eliminated with greater fidelity.

Here, we introduce the soft quantum control technique, in which the form of Rabi frequency can be chosen in a time-dependent Gaussian form that satisfies the condition of soft quantum control, which is small at the beginning and at the end of quantum evolution. First, time-independent Ω_1 can be changed into time-dependent Gaussian form $\Omega_1(t) = \Omega_m \exp[-(t-2T_1)^2/T_1^2]$ ($\Omega_1'(t) = \Omega_m \exp[-(t-2T_2)^2/T_2^2]$), we use $\Omega_1'(t)$ to express the Rabi frequency applied on target atoms when $U(\tau_2)$ is realized, where Ω_m and $T_{1,2}$ are the maximum amplitude and width of the Gaussian pulse, respectively. Second, according to the invariable pulse area $\int_0^{\tau_1}(\Omega_1^2/\delta)\mathrm{d}t = \pi$ ($\int_0^{\tau_2}(\Omega_1'^2/\delta)\mathrm{d}t = \pi/2$), the evolution time is determined as $T_1 = \tau_1/4 = 2\delta\pi/\sqrt{2\pi}\Omega_m^2$ ($T_2 = \tau_2/4 = \delta\pi/\sqrt{2\pi}\Omega_m^2$). Then, we can plot the population of evolution states, fidelity and average fidelity in fig. 3, fig. 4(a), and fig. 4(b), respectively, both fidelity and average fidelity can exceed 99.8% for $\hat{U}(\tau_1)$. And for $\hat{U}(\tau_2)$, the fidelity F and the average fidelity $\mathcal{F}$ can achieve 99.9% and 99.93%, separately.

Moreover, we also plot the fidelity solved by the Lindblad master equation

$$\dot{\rho} = -i[H_I, \rho] + \frac{\kappa}{2}\sum_{m=1}^{6}\mathcal{L}_1[\sigma_m] + \frac{\Gamma}{2}\sum_{n=1}^{3}\mathcal{L}_2[\nu_n] \qquad (11)$$

against decay (spontaneous emission of atoms) and dephasing in fig. 5 with time-independent Ω_1 in fig. 5(a) and time-dependent $\Omega_1(t)$ in fig. 5(b), where $\mathcal{L}[\mathcal{A}]$ are the Lindblad operators as $\mathcal{L}[\mathcal{A}] = 2\mathcal{A}\rho(t)\mathcal{A}^\dagger - \mathcal{A}^\dagger\mathcal{A}\rho(t) - \rho(t)\mathcal{A}^\dagger\mathcal{A}$ and

$$\begin{aligned}
\sigma_1 &= |1\rangle_1\langle r|,\ \sigma_2 = |0\rangle_1\langle r|,\ \sigma_3 = |1\rangle_2\langle r|,\\
\sigma_4 &= |0\rangle_2\langle r|,\ \sigma_5 = |1\rangle_3\langle r|,\ \sigma_6 = |0\rangle_3\langle r|,\\
\nu_1 &= |r\rangle_1\langle r| - |0\rangle_1\langle 0| - |1\rangle_1\langle 1|,\\
\nu_2 &= |r\rangle_2\langle r| - |0\rangle_2\langle 0| - |1\rangle_2\langle 1|,\\
\nu_3 &= |r\rangle_3\langle r| - |0\rangle_3\langle 0| - |1\rangle_3\langle 1|, \qquad (12)
\end{aligned}$$

κ is the decay rate of atoms caused by atomic decay and Γ is the dephasing rate of atoms.

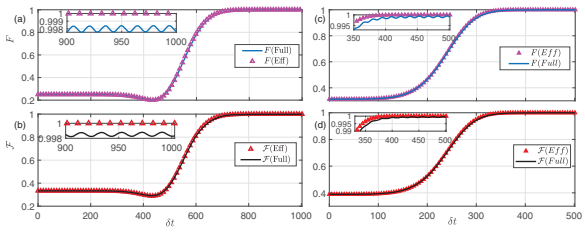

Fig. 4: The fidelity F ((a), (c)) and average fidelity $\mathcal{F}$ ((b), (d)) of the phase gate, where the purple (red) triangle and the blue (black) solid line denote the fidelity based on the effective Hamiltonian (eq. (6)) and the full Hamiltonian (eq. (1)), where $\Omega_m = 0.1\delta$ and the other parameters are the same as fig. 2.

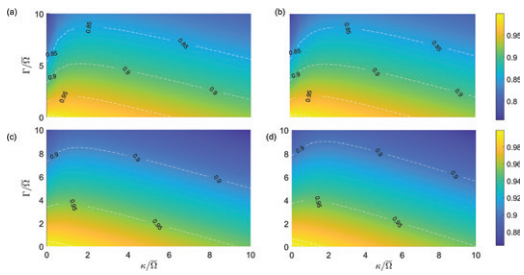

Fig. 5: Fidelity F *vs.* the spontaneous emission rate κ and the dephasing rate Γ of $U(\tau_1)$ without soft quantum control (a) and with soft quantum control (b), and $U(\tau_2)$ without soft quantum control (c) and with soft quantum control (d), where parameters are the same as fig. 4.

From fig. 5, we can find the fidelity influenced by the decay slightly, when the decay rate $\kappa/\overline{\Omega} = 6$ the fidelity can exceed 0.95 both without soft quantum control in fig. 5(a) and with soft quantum control in fig. 5(b) for $U(\tau_1)$, for $U(\tau_2)$, the fidelity can exceed 0.9 even if the spontaneous emission rate κ and the dephasing rate Γ are both high in figs. 5(c) and (d). Obviously, our proposal is insensitive to spontaneous emission due to virtual excitation. In addition, we can see that after applying soft quantum control, the robustness of this multiple-qubit entangled gate can be improved greatly.

In the experiment, the lifetime of the Rydberg state we select can reach ~ 1 ms [88]. The fidelity can achieve the maximum value within 99.77% (99.64%) even in the standard method without soft quantum control with $\Omega_m = 2\pi \times 0.1$ MHz. After applying soft quantum control, the fidelity of 99.9% (99.93%) can be achieved within 1 ms. As for the van der Walls interaction, the distance between control atom and target atoms is 9.0773 μm, and the distance of two target atoms is 12.8258 μm.

Conclusion. – We have proposed a method to realize multiple-qubit entangling gates based on URP by using off-resonant driving fields, which is insensitive to spontaneous emission because of the virtual excitation. Furthermore, Gaussian temporal modulation has been adopted to reduce the unwanted transitions, making it more robust to operation time errors. From numerical results, we find that our method based on soft quantum control achieves

extremely high fidelity to generate the entangling gate under achievable experimental parameters for which the fidelity is more stable and higher than the standard method. We believe that our scheme has great potential in realizing Rydberg quantum gates.

* * *

SLS acknowledges support from National Natural Science Foundation of China (NSFC) under Grant No.12274376 and Major science and technology project of Henan Province under Grant No. 221100210400. LL acknowledges support from National Natural Science Foundation of China (NSFC) under Grant No. 11804375 and 12074346, and Natural Science Foundation of Henan Province under Grant No. 212300410085. YJ acknowledges support from National Natural Science Foundation of China (NSFC) under Grant No. 11774078 and 12074099. SC acknowledges support from Shanghai Municipal Science and Technology Fundamental Project under Grant No. 21JC1405400.

Data availability statement: The data that support the findings of this study are available upon reasonable request from the authors.

Appendix

Here, we will introduce the classification of three-qubit states. It has been shown that there are only two kinds of genuine entangled three-qubit states: GHZ class and W class states. Here we prove that the prepared states based on eq. (8) belong to the GHZ class by using the criterion obtained in [89,90].

First, any pure three-qubit state can be expressed as

$$\begin{aligned}|\psi\rangle = \; & a_0|000\rangle + a_1|001\rangle + a_2|010\rangle + a_3|011\rangle \\ & + a_4|100\rangle + a_5|101\rangle + a_6|110\rangle + a_7|111\rangle,\end{aligned} \tag{A.1}$$

with $\sum_i |a_i|^2 = 1$. Then, the state belongs to the GHZ class state if and only if it can be converted into the standard GHZ state $\frac{1}{\sqrt{2}}(|000 + |111\rangle)$ under proper stochastic local operation and classical communication (SLOCC). Mathematically, one sufficient and necessary condition for $|\Psi\rangle$ being a GHZ-class state is [90]

$$\begin{aligned}&(a_0a_7 - a_2a_5 + a_1a_6 - a_3a_4)^2 \\ &-4(a_2a_4 - a_0a_6)(a_3a_5 - a_1a_7) \neq 0.\end{aligned} \tag{A.2}$$

Obviously, $|\Psi(\tau_1)\rangle(|\Psi(\tau_2)\rangle)$ satisfies this condition. So, $|\Psi(\tau_1)\rangle(|\Psi(\tau_2)\rangle)$ is equivalent to GHZ state under SLOCC.

REFERENCES

[1] Ekert A. K., *Phys. Rev. Lett.*, **67** (1991) 661.
[2] Schimpf C., Reindl M., Huber D., Lehner B., Silva S. F. C. D., Manna S., Vyvlecka M., Walther P. and Rastelli A., *Sci. Adv.*, **7** (2021) eabe8905.
[3] Bennett C. H. and Wiesner S. J., *Phys. Rev. Lett.*, **69** (1992) 2881.
[4] Wu J., Long G.-L. and Hayashi M., *Phys. Rev. Appl.*, **17** (2022) 064011.
[5] Bennett C. H., Brassard G., Crépeau C., Jozsa R., Peres A. and Wootters W. K., *Phys. Rev. Lett.*, **70** (1993) 1895.
[6] Karlsson A. and Bourennane M., *Phys. Rev. A*, **58** (1998) 4394.
[7] Cirac J. I., Ekert A. K., Huelga S. F. and Macchiavello C., *Phys. Rev. A*, **59** (1999) 4249.
[8] Yun M., Guo F.-Q., Li M., Yan L.-L., Feng M., Li Y.-X. and Su S.-L., *Opt. Express*, **29** (2021) 8737.
[9] Hillery M., Bužek V. and Berthiaume A., *Phys. Rev. A*, **59** (1999) 1829.
[10] Xiao L., Lu Long G., Deng F.-G. and Pan J.-W., *Phys. Rev. A*, **69** (2004) 052307.
[11] Cerf N. J., Bourennane M., Karlsson A. and Gisin N., *Phys. Rev. Lett.*, **88** (2002) 127902.
[12] Jo Y. and Son W., *Phys. Rev. A*, **94** (2016) 052316.
[13] Shor P. W. and Preskill J., *Phys. Rev. Lett.*, **85** (2000) 441.
[14] Lo H.-K., Ma X. and Chen K., *Phys. Rev. Lett.*, **94** (2005) 230504.
[15] Shen C.-P., Xiu X.-M., Dong L., Zhu X.-Y., Chen L., Liang E., Yan L.-L. and Su S.-L., *Ann. Phys. (Berlin)*, **531** (2019) 1900160.
[16] Song C., Xu D., Zhang P., Wang J., Guo Q., Liu W., Xu K., Deng H., Huang K., Zheng D., Zheng S.-B., Wang H., Zhu X., Lu C.-Y. and Pan J.-W., *Phys. Rev. Lett.*, **121** (2018) 030502.
[17] Zhu Q., Cao S., Chen F., Chen M.-C., Chen X., Chung T.-H., Deng H., Du Y., Fan D., Gong M., Guo C., Guo C., Guo S., Han L., Hong L., Huang H.-L., Huo Y.-H., Li L., Li N., Li S., Li Y., Liang F., Lin C., Lin J., Qian H., Qiao D., Rong H., Su H., Sun L., Wang L., Wang S., Wu D., Wu Y., Xu Y., Yan K., Yang W., Yang Y., Ye Y., Yin J., Ying C., Yu J., Zha C., Zhang C., Zhang H., Zhang K., Zhang Y., Zhao H., Zhao Y., Zhou L., Lu C.-Y., Peng C.-Z., Zhu X. and Pan J.-W., *Sci. Bull.*, **67** (2022) 240.
[18] Gong M., Wang S., Zha C., Chen M.-C., Huang H.-L., Wu Y., Zhu Q., Zhao Y., Li S., Guo S., Qian H., Ye Y., Chen F., Ying C., Yu J., Fan D., Wu D., Su H., Deng H., Rong H., Zhang K., Cao S., Lin J., Xu Y., Sun L., Guo C., Li N., Liang F., Bastidas V. M., Nemoto K., Munro W. J., Huo Y.-H., Lu C.-Y., Peng C.-Z., Zhu X. and Pan J.-W., *Science*, **372** (2021) 948.
[19] Wu Y., Bao W.-S., Cao S., Chen F., Chen M.-C., Chen X., Chung T.-H., Deng H., Du Y., Fan D., Gong M., Guo C., Guo C., Guo S., Han L., Hong L., Huang H.-L., Huo Y.-H., Li L., Li N., Li S., Li Y., Liang F., Lin C., Lin J., Qian H., Qiao D., Rong H., Su H., Sun L., Wang L., Wang S., Wu D., Xu Y., Yan K., Yang W., Yang Y., Ye Y., Yin J., Ying C., Yu J., Zha C., Zhang C., Zhang H., Zhang K., Zhang Y., Zhao H., Zhao Y., Zhou L., Zhu Q., Lu C.-Y., Peng C.-Z., Zhu X. and Pan J.-W., *Phys. Rev. Lett.*, **127** (2021) 180501.
[20] Bremner M. J., Dawson C. M., Dodd J. L., Gilchrist A., Harrow A. W., Mortimer D., Nielsen

M. A. and Osborne T. J., *Phys. Rev. Lett.*, **89** (2002) 247902.
[21] Nielsen M. A. and Chuang I., *Am. J. Phys.*, **70** (2002) 558.
[22] Barenco A., Bennett C. H., Cleve R., DiVincenzo D. P., Margolus N., Shor P., Sleator T., Smolin J. A. and Weinfurter H., *Phys. Rev. A*, **52** (1995) 3457.
[23] Wei L. F., Liu Y.-x. and Nori F., *Phys. Rev. Lett.*, **96** (2006) 246803.
[24] Cervera-Lierta A., Krenn M., Aspuru-Guzik A. and Galda A., *Phys. Rev. Appl.*, **17** (2022) 024062.
[25] Han J.-X., Wu J.-L., Wang Y., Xia Y., Jiang Y.-Y. and Song J., *Phys. Rev. B*, **105** (2022) 064431.
[26] Foss-Feig M., Ragole S., Potter A., Dreiling J., Figgatt C., Gaebler J., Hall A., Moses S., Pino J., Spaun B., Neyenhuis B. and Hayes D., *Phys. Rev. Lett.*, **128** (2022) 150504.
[27] Shao X. Q., Wu J. H., Yi X. X. and Long G.-L., *Phys. Rev. A*, **96** (2017) 062315.
[28] Su S. L., Shen H. Z., Liang E. and Zhang S., *Phys. Rev. A*, **98** (2018) 032306.
[29] He Y., Liu J.-X., Guo F.-Q., Yan L.-L., Luo R., Liang E., Su S.-L. and Feng M., *Opt. Commun.*, **505** (2022) 127500.
[30] Li M., Li J.-Y., Guo F.-Q., Zhu X.-Y., Liang E., Zhang S., Yan L.-L., Feng M. and Su S.-L., *Ann. Phys. (Berlin)*, **534** (2022) 2100506.
[31] Guo F., Zhu X.-Y., Yun M.-R., Yan L.-L., Zhang Y., Jia Y. and Su S., *EPL*, **137** (2022) 55001.
[32] Monz T., Schindler P., Barreiro J. T., Chwalla M., Nigg D., Coish W. A., Harlander M., Hänsel W., Hennrich M. and Blatt R., *Phys. Rev. Lett.*, **106** (2011) 130506.
[33] Gallagher T. F., *Rydberg Atoms, Cambridge Monographs on Atomic, Molecular and Chemical Physics Book 3* (Cambridge University Press) 2005.
[34] Saffman M., Walker T. G. and Mølmer K., *Rev. Mod. Phys.*, **82** (2010) 2313.
[35] Urban E., Johnson T. A., Henage T., Isenhower L., Yavuz D. D., Walker T. G. and Saffman M., *Nat. Phys.*, **5** (2009) 110.
[36] Gaëtan A., Miroshnychenko Y., Wilk T., Chotia A., Viteau M., Comparat D., Pillet P., Browaeys A. and Grangier P., *Nat. Phys.*, **5** (2009) 115.
[37] Béguin L., Vernier A., Chicireanu R., Lahaye T. and Browaeys A., *Phys. Rev. Lett.*, **110** (2013) 263201.
[38] Wu J.-L., Wang Y., Han J.-X., Jiang Y., Song J., Xia Y., Su S.-L. and Li W., *Phys. Rev. Appl.*, **16** (2021) 064031.
[39] Møller D., Madsen L. B. and Mølmer K., *Phys. Rev. Lett.*, **100** (2008) 170504.
[40] Su S. L., *Chin. Phys. B*, **27** (2018) 110304.
[41] Shi X.-F., *Phys. Rev. Appl.*, **14** (2020) 054058.
[42] Shi X.-F., *Phys. Rev. Appl.*, **11** (2019) 044035.
[43] Young J. T., Bienias P., Belyansky R., Kaufman A. M. and Gorshkov A. V., *Phys. Rev. Lett.*, **127** (2021) 120501.
[44] Petrosyan D., Motzoi F., Saffman M. and Mølmer K., *Phys. Rev. A*, **96** (2017) 042306.
[45] Beterov I. I., Ashkarin I. N., Yakshina E. A., Tretyakov D. B., Entin V. M., Ryabtsev I. I., Cheinet P., Pillet P. and Saffman M., *Phys. Rev. A*, **98** (2018) 042704.
[46] Mitra A., Martin M. J., Biedermann G. W., Marino A. M., Poggi P. M. and Deutsch I. H., *Phys. Rev. A*, **101** (2020) 030301.
[47] Khazali M. and Mølmer K., *Phys. Rev. X*, **10** (2020) 021054.
[48] Saffman M., Beterov I. I., Dalal A., Páez E. J. and Sanders B. C., *Phys. Rev. A*, **101** (2020).
[49] Isenhower L., Urban E., Zhang X. L., Gill A. T., Henage T., Johnson T. A., Walker T. G. and Saffman M., *Phys. Rev. Lett.*, **104** (2010) 010503.
[50] Maller K. M., Lichtman M. T., Xia T., Sun Y., Piotrowicz M. J., Carr A. W., Isenhower L. and Saffman M., *Phys. Rev. A*, **92** (2015) 022336.
[51] Levine H., Keesling A., Semeghini G., Omran A., Wang T. T., Ebadi S., Bernien H., Greiner M., Vuletić V., Pichler H. and Lukin M. D., *Phys. Rev. Lett.*, **123** (2019) 170503.
[52] Saffman M. and Mølmer K., *Phys. Rev. Lett.*, **102** (2009) 240502.
[53] Zhu X.-Y., Jin Z., Liang E., Zhang S. and Su S.-L., *Ann. Phys. (Berlin)*, **532** (2020) 2000059.
[54] Beterov I. I., Hamzina G. N., Yakshina E. A., Tretyakov D. B., Entin V. M. and Ryabtsev I. I., *Phys. Rev. A*, **97** (2018) 032701.
[55] Zhang X. L., Isenhower L., Gill A. T., Walker T. G. and Saffman M., *Phys. Rev. A*, **82** (2010) 030306.
[56] Wilk T., Gaëtan A., Evellin C., Wolters J., Miroshnychenko Y., Grangier P. and Browaeys A., *Phys. Rev. Lett.*, **104** (2010) 010502.
[57] Zeng Y., Xu P., He X., Liu Y., Liu M., Wang J., Papoular D. J., Shlyapnikov G. V. and Zhan M., *Phys. Rev. Lett.*, **119** (2017) 160502.
[58] Levine H., Keesling A., Omran A., Bernien H., Schwartz S., Zibrov A. S., Endres M., Greiner M., Vuletić V. and Lukin M. D., *Phys. Rev. Lett.*, **121** (2018) 123603.
[59] Graham T. M., Kwon M., Grinkemeyer B., Marra Z., Jiang X., Lichtman M. T., Sun Y., Ebert M. and Saffman M., *Phys. Rev. Lett.*, **123** (2019) 230501.
[60] Madjarov I. S., Covey J. P., Shaw A. L., Choi J., Kale A., Cooper A., Pichler H., Schkolnik V., Williams J. R. and Endres M., *Nat. Phys.*, **16** (2020) 857.
[61] Lukin M. D., Fleischhauer M., Cote R., Duan L. M., Jaksch D., Cirac J. I. and Zoller P., *Phys. Rev. Lett.*, **87** (2001) 037901.
[62] Kang Y.-H., Shi Z.-C., Song J. and Xia Y., *Phys. Rev. A*, **102** (2020) 022617.
[63] Su S.-L., Guo F.-Q., Tian L., Zhu X.-Y., Yan L.-L., Liang E.-J. and Feng M., *Phys. Rev. A*, **101** (2020) 012347.
[64] Ates C., Pohl T., Pattard T. and Rost J. M., *Phys. Rev. Lett.*, **98** (2007) 023002.
[65] Amthor T., Giese C., Hofmann C. S. and Weidemüller M., *Phys. Rev. Lett.*, **104** (2010) 013001.
[66] Su S.-L., Tian Y., Shen H. Z., Zang H., Liang E. and Zhang S., *Phys. Rev. A*, **96** (2017) 042335.
[67] Su S.-L., Gao Y., Liang E. and Zhang S., *Phys. Rev. A*, **95** (2017) 022319.

[68] Su S.-L., Liang E., Zhang S., Wen J.-J., Sun L.-L., Jin Z. and Zhu A.-D., *Phys. Rev. A*, **93** (2016) 012306.
[69] Su S.-L., Guo F.-Q., Wu J.-L., Jin Z., Shao X. Q. and Zhang S., *EPL*, **131** (2020) 53001.
[70] Li D. X. and Shao X. Q., *Phys. Rev. A*, **98** (2018) 062338.
[71] Haase J. F., Wang Z.-Y., Casanova J. and Plenio M. B., *Phys. Rev. Lett.*, **121** (2018) 050402.
[72] Han J.-X., Wu J.-L., Wang Y., Xia Y., Jiang Y.-Y. and Song J., *Phys. Rev. A*, **103** (2021) 032402.
[73] Li D.-X., Yang C. and Shao X.-Q., *Quantum Eng.*, **3** (2021) e66.
[74] Pezzagna S. and Meijer J., *Appl. Phys. Rev.*, **8** (2021) 011308.
[75] Wang Z.-Y., Lang J. E., Schmitt S., Lang J., Casanova J., McGuinness L., Monteiro T. S., Jelezko F. and Plenio M. B., *Phys. Rev. Lett.*, **122** (2019) 200403.
[76] Yin H.-D. and Shao X.-Q., *Opt. Lett.*, **46** (2021) 2541.
[77] Isenhower L., Urban E., Zhang X. L., Gill A. T., Henage T., Johnson T. A., Walker T. G. and Saffman M., *Phys. Rev. Lett.*, **104** (2010) 010503.
[78] Zhang X. L., Isenhower L., Gill A. T., Walker T. G. and Saffman M., *Phys. Rev. A*, **82** (2010) 030306.
[79] Dudin Y. O. and Kuzmich A., *Science*, **336** (2012) 887.
[80] Barredo D., Lienhard V., Scholl P., de Léséleuc S., Boulier T., Browaeys A. and Lahaye T., *Phys. Rev. Lett.*, **124** (2020) 023201.
[81] Levine H., Keesling A., Semeghini G., Omran A., Wang T. T., Ebadi S., Bernien H., Greiner M., Vuletić V., Pichler H. and Lukin M. D., *Phys. Rev. Lett.*, **123** (2019) 170503.
[82] Wu J.-L., Su S.-L., Wang Y., Song J., Xia Y. and Jiang Y.-Y., *Opt. Lett.*, **45** (2020) 1200.
[83] Weber S., Tresp C., Menke H., Urvoy A., Firstenberg O., Büchler H. P. and Hofferberth S., *J. Phys. B: At. Mol. Opt. Phys.*, **50** (2017) 133001.
[84] Li D.-X., Zheng T.-Y. and Shao X.-Q., *Opt. Express*, **27** (2019) 20874.
[85] James D. F. and Jerke J., *Can. J. Phys.*, **85** (2007) 625.
[86] Nielsen M. A., *Phys. Lett. A*, **303** (2002) 249.
[87] Mowbray C. T., Holter M. C., Teague G. B. and Bybee D., *Am. J. Eval.*, **24** (2003) 315.
[88] Beterov I. I., Ryabtsev I. I., Tretyakov D. B. and Entin V. M., *Phys. Rev. A*, **79** (2009) 052504.
[89] Bennett C. H., Popescu S., Rohrlich D., Smolin J. A. and Thapliyal A. V., *Phys. Rev. A*, **63** (2000) 012307.
[90] Li D., Li X., Huang H. and Li X., *Phys. Lett. A*, **359** (2006) 428.